The Korean Institute of Communications and Information Sciences

Available online at www.sciencedirect.com

ScienceDirect

ICT Express 8 (2022) 626–632

www.elsevier.com/locate/icte

Temperature monitoring techniques of power cable joints in underground utility tunnels using a fiber Bragg grating

Hyunjin Kim*, Misuk Lee, Woo-Sug Jung, Seung-Hee Oh

Electronics and Telecommunications Research Institute, Daejeon, Republic of Korea

Received 28 April 2022; received in revised form 4 July 2022; accepted 17 July 2022
Available online 23 July 2022

Abstract

Underground utility tunnels (UUTs), facilities where utilities such as electricity, gas, and telecommunication are concentrated, constitute important infrastructures that help humans with their daily lives. Therefore, it is of utmost importance to protect UUTs from disasters. Power cable accidents in UUT internal facilities mostly occur at the joints of power cables. This paper proposes a temperature sensor module for detecting fires (a disaster that can occur in UUTs) that may occur at the "cable joints" of cables used in a power distribution grid. Long-distance transmission is possible without interference from electromagnetic waves as the proposed temperature sensor module is based on a fiber optic sensor. Therefore, it is suitable for application in narrow and long UUTs. When light from a broadband light source is sent to the fiber Bragg grating (FBG), signals with different wavelengths according to the temperature are reflected. The optical filter module divides the reflected signal into four wavelengths and demodulates it simultaneously. The signal demodulated through self-referencing had an almost linear characteristic. The adjusted R-squared value, indicating the degree of linearity, was $\geq$0.99744, and the temperature resolution of the analysis module was 1 °C. We placed the proposed FBG on an energized cable joint of the power distribution grid and measured the temperature. Herein, we present the configuration of the sensor module and the measured results.

Keywords: Power cable monitoring; Fiber Bragg grating; Optical temperature sensor; Underground utility tunnel

1. Introduction

Essential services such as power, telecommunications, water, and gas are transported and supplied using underground utility tunnels (UUTs) in densely populated areas such as a city. A UUT is an important infrastructure since various utilities and services that are necessary for the sustenance of life are installed and managed in it.

In 2018, a fire occurred in an ancillary facility rather than in the pipelines of an telecommunications cable tunnel in Seoul, South Korea. Wired and wireless telephones were out of service, and security and medical facilities and telecommunications services, such as cards and automated teller machines (ATMs), were blocked. The lost portion of the telecommunication cable, which was originally 150 m in length, was 79 m in length. This incident resulted in the loss of millions of dollars, and the uncounted losses are estimated to be even greater. Moreover, UUTs are often installed in areas where industrial facilities are clustered. In this case, the loss cost due to the disaster or accident will increase exponentially.

Generally, two or more different types of cables or pipelines are accommodated in one UUT. Therefore, when a disaster (accident) occurs in one of them, it can spread to others nearby. For example, if power and telecommunication cables are close to each other and an explosion or fire occurs in the power cable, there is a high probability that an accident will also occur in the telecommunication cable.

The Korean government recognized the need for upgrading the UUT management system, and in 2020, four ministries initiated the "Digital Twin-Based Underground Public Tunnel Fire and Disaster Management Integrated Platform Technology Development" project [1].

Several sensors are used to monitor the status of accommodated facilities in the UUT. For example, optical and acoustic sensors are used to monitor gas and water pipes [2,3], while partial discharge and temperature sensors are used to monitor power cables [4–6]. The Korea fire safety standard document, KFS 1252 (fire safety standards for a UUT), presents the history of fires in UUTs that have occurred in Korea since

* Corresponding author.
E-mail addresses: hjkim80@etri.re.kr (H. Kim), lms@etri.re.kr (M. Lee), wsjung@etri.re.kr (W.-S. Jung), seunghee5@etri.re.kr (S.-H. Oh).

Peer review under responsibility of The Korean Institute of Communications and Information Sciences (KICS).

https://doi.org/10.1016/j.icte.2022.07.006

1993. According to this document, for the telecommunication sector, the possibility of fire is higher in the ancillary facilities than in the telecommunication cable itself. For water pipes, it is possible to identify if there is an abnormality through the specific vibration or sound generated in the pipe by patrol. However, in the case of power cables, checking whether there is an abnormality by patrolling is difficult.

Herein, we propose a sensor for diagnosing the anomalies of power cables. Power cables are typically several kilometers or longer, making it difficult to monitor them entirely. Nakamura [5] reported that the cable joint, which is the junction of different power cables, is where most accidents in a power cable occur. Moreover, we need to monitor the cable joint without interrupting the power. In this case, the available diagnostic methods are partial discharge or temperature measurement. Electromagnetic waves can affect and distort the signals of thermocouples, which are commonly used as temperature sensors. UUTs can be narrow and long, requiring signals to be transmitted several kilometers in the same space as power cables that emit strong electromagnetic waves.

Fiber optic sensors can measure from a far distance without electromagnetic interference [7]. FBG is a quasi-distributed fiber optic sensor that can inscribe a Bragg grating at the required location on the fiber. This is advantageous when manufacturing the sensor according to the irregular position of the cable joint.

However, FBG sensors require demodulation and expensive instruments. For example, the purchase cost of the optical spectrum analyzer (OSA) is over 10,000 dollars, and Ibsen's interrogator for FBG costs 3500 euros. However, experts at Electric Power suggested that we did not require high precision; hence, we focused on reducing the production cost. A used filter costs <25 dollars. In addition, it is a passive device whose breakdowns are fewer than those of an active device. This is expected to be advantageous for the field application of the optical sensor.

Herein, we propose a sensor module that simultaneously demodulates the wavelengths of four different FBGs by combining optical filters. In addition, we present the measurement results of the temperature change of the cable joint of the manhole, which is a structure similar to that of a UUT, using the proposed sensor module.

2. System setup and specification

2.1. Optical component

An FBG is a component in which a refractive index change is periodically applied inside an optical fiber, such as a grating [8]. According to the spacing of the grating, a specific wavelength signal is reflected, and the other signals are transmitted. The reflected wavelength is shifted based on the temperature or strain applied to the FBG. To demodulate an FBG, various techniques have been studied; these include the use of wavelength analysis equipment such as OSA, a filter with different transmittances depending on the wavelength such as LTF, a tunable filter or laser, an interferometer, or a photodetector array [8–14]. LTF is used to tune the intensity of a reflected FBG signal by wavelength. Tunable filters or lasers convert wavelengths into the time domain. For example, if sweeping is performed for 10 s with the same speed in the range of 1550–1560 nm, the wavelength value confirmed at 5 s will be 1555 nm.

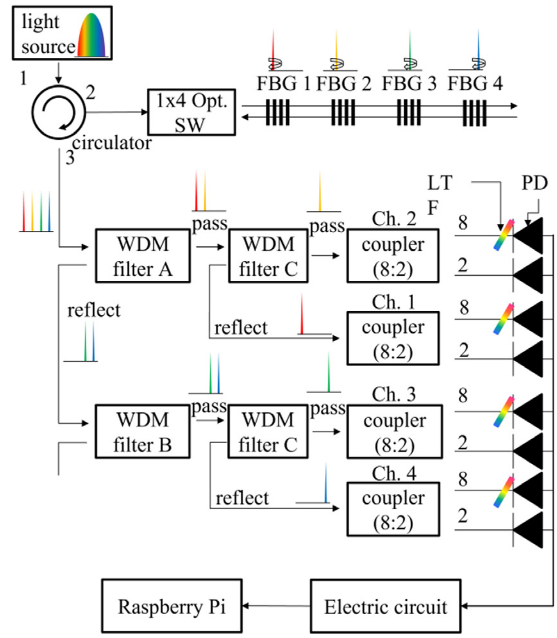

Fig. 1. Schematic of the proposed module. WDM is wavelength division multiplexing.

The proposed module measures the amount of light that is changed by the temperature or strain. However, the amount of light can also be changed through external stimulation applied to the optical fiber. To overcome this, a structure in which the FBG signal is divided by the reference signal was applied [14]. Fig. 1 shows a schematic illustration of the proposed module.

One of the diagnostic methods for assessing power cables is checking whether there is a temperature difference of >10° between each phase of the cable. This varies from country to country and is the standard used in Korea. Therefore, it is necessary to install a temperature sensor for each phase and compare the temperature for each phase. To demodulate multiple sensors, we combined three types of WDM filters, each corresponding to a different wavelength band. The filter passes for the different wavelength bands are 1540–1560 (WDM filter A), 1560–1580 (WDM filter B), and 1550–1570 nm (WDM filter C). A filter pass is a passive component in the form of a steel tube and consists of three ports: com, pass, and reflection. All wavelength properties are shown in Fig. 2. The optical signal was divided into four wavelength bands by passing through the combined WDM filter. Subsequently, it was divided into sensor and reference signals at an 8:2 ratio. The sensor signal passed through a linear transmitter filter (LTF). The temperature was measured by analyzing the change in the amount of light passing through the LTF. The optical characteristics of the LTF transmitted linearly within the ranges of 1541–1548, 1551–1558, 1561–1568, and 1571–1578 nm. The LTFs are attached to the end of the angled physical contact (APC)

Table 1
Specifications of the WDM filter.

Parameter		WDM filter A	WDM filter B	WDM filter C
Pass channel wavelength range		1550 ± .75	1570 ± .75	1545 ± .2
Reflect channel wavelength range		1260–1537.5 & 1562.5–1620	1260–1557.5 & 1582.5–1620	
Insertion loss (dB)	Pass channel	0.40	50.45	0.42
	Reflect channel	0.33	70.25	80.21
Isolation (dB)	Pass channel	36	34	49
	Reflect channel	20	20	19
PDL (dB)	Pass channel	0.04	0.04	0.04
	Reflect channel	0.05	0.04	0.06
Return loss (dB)		51	49	55
Fiber type		SMF-28e with a 900 um loose tube	SMF-28e with a 900 um loose tube	SMF-28e with a 900 um loose tube

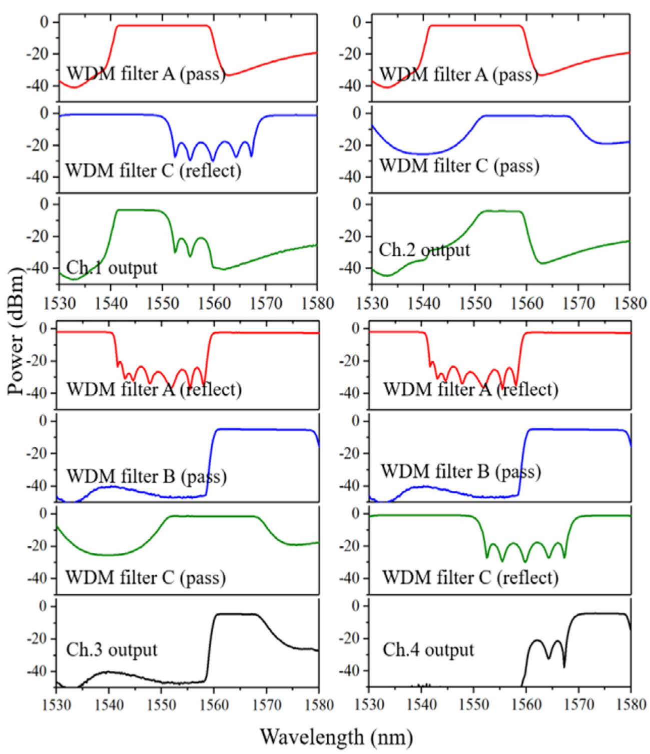

Fig. 2. Filtered wavelength by the WDM filter combination. Ch. 1: WDM A (pass) & WDM C (reflect), Ch. 2: WDM A (pass) & WDM C (pass), Ch. 3: WDM A (reflect) & WDM B (pass) & WDM C (pass), Ch. 4: WDM A (reflect) & WDM B (pass), & WDM C (reflect).

ferrule and assembled with the photo-detector (PD). Table 1 lists the specification of WDM filters.

Fig. 2 shows the wavelengths of optical filters. We measured wavelengths using an OSA. The wavelength band passing through WDM filter A was 1540–1560 nm. The wavelength bands were divided into 1540–1550 and 1550–1560 by applying WDM filter C to the primary filtered signal. The outputs of channels 1 and 2 shown in Fig. 2 show the results. In a similar process, the wavelength bands of 1560–1570 and 1570–1580 nm were separated.

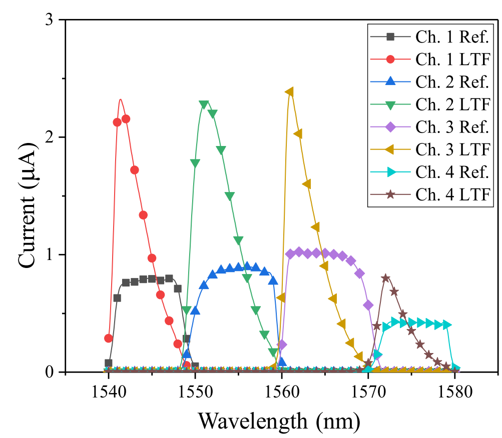

Fig. 3. Spectra of the wavelength divided by WDM filters and the LTF. LTF: Linear transmittance filter output; Ref: reference output.

Table 2
Parameters of linear regression analysis.

Channel	Ch. 1	Ch. 2	Ch. 3	Ch. 4
Slope	−0.51011	−0.46228	−0.34812	−0.38648
Intercept	789.31986	720.10967	545.67669	609.50736
R-square	0.99864	0.99955	0.99862	0.99756
Adj. R-square	0.99857	0.99953	0.99855	0.99744

A graph is presented in Fig. 3 to confirm the final characteristics when the optical signal reflected from the FBG passes through the combined optical filter.

As the spectrum of a laser is similar to the reflected wavelength of the FBG, the wavelength of the laser was changed in units of 0.1 nm to confirm the output characteristics. A tunable laser source, current source meter, and laptop related to a general-purpose interface bus (GPIB) cable were used. A tunable laser source was connected to port 2 of the circulator and was swept at 0.1 nm intervals and 50 μW in the range of 1540 to 1580 nm. The laser signal was similar to the FBG reflection. We controlled the laser and measured the output using the LabVIEW program. During optical module manufacturing, some distortions occurred in the output due to splicing, bending loss, and filter bonding. (See Table 2.)

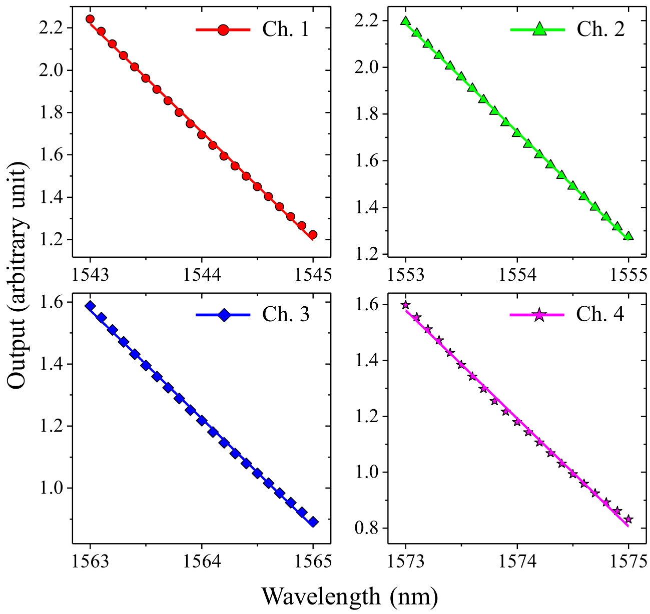

Fig. 4. Final output and linear fitting of four channels.

According to the study conducted by Y. Sano [15], a part of the linear output of array waveguide grating (AWG) could be used as LTF. Similarly, at each channel, approximately 2–3 nm among 10 nm is linear. In Fig. 4, only 2 nm is used. Fig. 4 shows the output to divide the LTF signal by the reference signal in the linear range, which is same with data presented in Fig. 3. For each channel, we applied the linear regression analysis on the final output. According to the linear regression analysis of Ch. 4, the R-squared and adjusted R-squared are 0.99756 and 0.99744, respectively. R-squared is an indicator of how close it is to linearity. The adjusted R-squared was used since the R-squared continuously increases as the number of variables increases. The worst value of R-squared was 0.99744, which can be almost linear. This means that the output of the optical filter module responded linearly to the FBG of four channels.

The light source was pOA, which is a small-sized commercial Erbium-doped fiber amplifier (EDFA) with an output power of 5 dBm and wavelength range of 1523–1563 nm. Channels 3 and 4 were out of the wavelength range of the light source, but the specifications were based on a 3-dB bandwidth. The optical power was sufficient for practical use.

The center wavelengths of the FBG sensors are 1544, 1554, 1564, and 1574 nm, while the reflectivity and 3-dB band width are 90% and ~0.25 nm, respectively.

2.2. Module housing

The final output of the optical component is the current of the PD. In this process, an optical signal is converted into an electrical signal. It is necessary to convert this into a temperature value such that the user can use it. The conversion process was performed using an electrical circuit and microprocessor.

Fig. 5 shows the manufactured module. The optical filter module is located at the bottom, and an electronic circuit for PD, light source, and a 1 × 4 optical switch are above it. The 1 × 4 optical switch was prepared for the case where there are many measurement points. In this experiment, only one channel was used. The presence or absence of a switch has no effect. If multiple measurements are required, we can use up to sixteen FBGs. A Raspberry Pi was placed on the optical components and electric circuit. The optical signal was converted into an electric signal by the electrical circuit, consisting of several resistors, capacitors, and integrated circuit (IC) chips. A 16-bit analog-to-digital converter (ADC) was used for the PD. The Raspberry Pi was used for sensor data acquisition, the temperature conversion of the output of the optical filter module, and communication. The temperature resolution can be finer, but it was set to 1 °C, based on the requirements of the user. Fig. 6 illustrates the measurement results of channel 1 at room temperature. Measurements were made indoors without any significant temperature change.

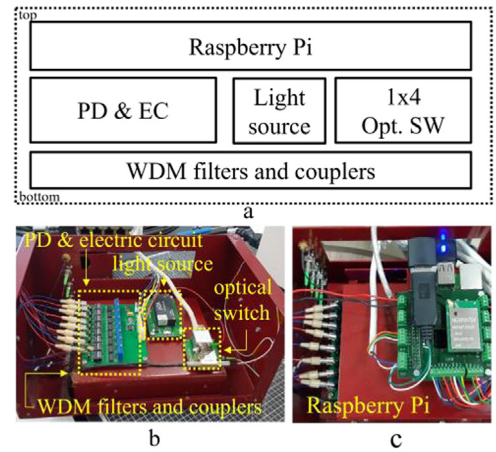

Fig. 5. Manufactured module. a. Module block diagram; b. optical component and electric circuit; and c. microcontroller.

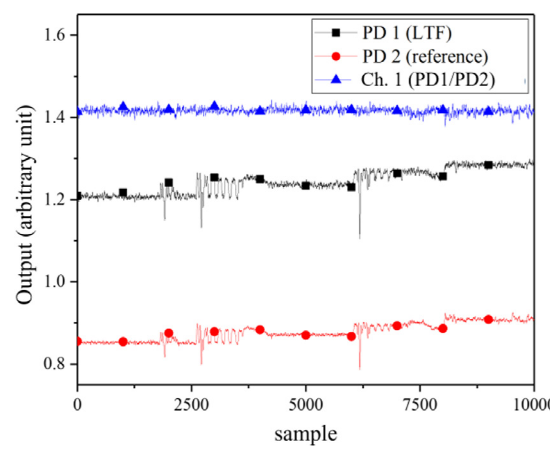

Fig. 6. Output at room temperature.

FBGs were attached to the hot plate and covered with a plastic lid to minimize external temperature disturbances. There was no temperature change, but the output was fluctuating. The distortion of the sensor output was due to fluctuations in the light source power and disturbances in the optical fiber.

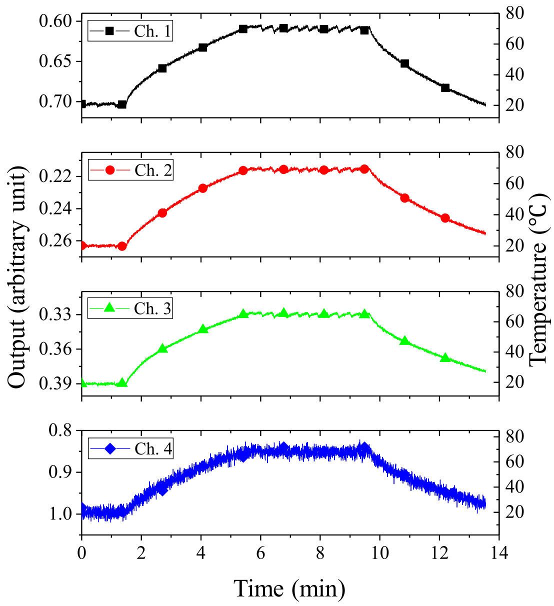

Fig. 7. PD Output with temperature change.

By LTF signal divided by the reference signal, the distortion caused by the light source and optical fiber was compensated. In Fig. 6, the final optical signal is almost stable compared to those of PD 1 and PD 2 based on the output of channel 1.

Fig. 7 shows the measurement results of temperature variation.

The test was performed at room temperature (approximately 24 °C). There was no temperature change during the first 2 min. The hot plate temperature was set to 80 °C for approximately 9 min, in which it took about 4 min to reach 80 °C. Channel 4 was noisier than the other channels because the output of the wavelength band emitted from the light source was low. After the temperature of the hot plate reached 80 °C, a temperature change was observed in the form of a sawtooth, without the sawtooth being allowed to become flat by controlling the hot plate temperature. A temperature chamber was used for system temperature calibration.

In UUT, almost power cables consist of three cables with a phase difference of 120°, indicating that it is enough to measure the temperature of all cables with Ch 1, 2, and 3. Channel 4, which is relatively noisy, can be used as a spare.

The manufactured device was designed to be waterproof; therefore, it was difficult for the internal heat to escape to the outside. The internal temperature was expected to gradually increase because of the closed-system conditions. The system was placed in a temperature chamber and heated up to 90 °C to confirm the operation simulation at high temperatures, during which the file-copy process was performed to apply a load to the microprocessor. No issues were observed at 80 °C, but rebooting sometimes occurred at 90 °C. The internal temperature rarely increased to 80 °C unless there was a fire. Thus, the device is expected to operate without any problems, even during the hot summer season.

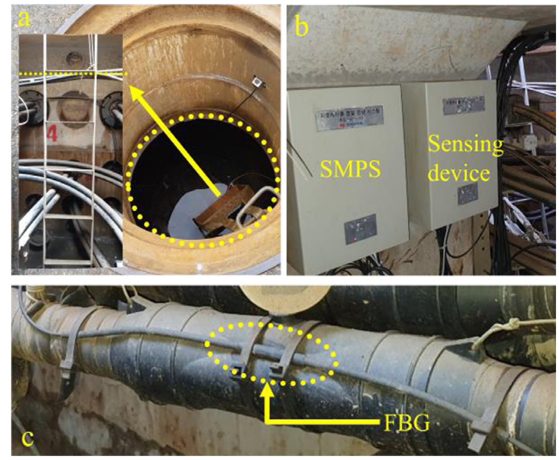

Fig. 8. On-site device installation. a. On-site manhole, b. power module and sensing device, and c. FBG on a power cable joint.

2.3. On-site temperature monitoring

To confirm the reliability of the equipment, A field test was performed on the manhole of an underground distribution grid, which was a worse condition than the UUT. Fig. 8 shows the installation of the proposed system in an actual manhole.

Fig. 8 illustrates the installation of the proposed system in an actual manhole. Manholes are often filled with water because of the presence of various electrical parts; thus, waterproofing was essential. The target manhole was filled with water near the entrance, as shown in Fig. 8a. In Fig. 8b, the left and right enclosures contain a switching mode power supply (SMPS) and the proposed module, respectively. Therefore, power was not supplied inside the manhole. When current flowed through the power cable, a magnetic field was generated, and power was supplied using the power current transformer (CT), which is a device that converts electromagnetic waves into electrical power. The measured data were transmitted to power line communication. If used in the UUT, the proposed module could be in the facility room or control room; therefore, the supply power through the SMPS or power line communication (PLC) was not required. In this study, the installation location was selected based on the harshness of the environment. Therefore, a power supply or communication network was required. Consequently, we employed an SMPS and a PLC. We installed an FBG on the power cable surface, as shown in Fig. 8c. However, most field workers are not familiar with FBG sensors. Therefore, the optical fiber had to be durable to prevent damage to the optical fiber sensor due to user negligence. An 'armored cable' was also used for additional protection of the FBG. Inside the cable, a metal spring structure surrounds the optical fiber. The shape of the manhole varies depending on the cable arrangement and environment, and the manhole where the system is installed has an L-shape. Since there was no power terminal in the manhole, a device for self-generation was installed for the experiment.

Fig. 9 shows the measured temperature of the cable surface from 0:00 to 23:00. The resistance component of the power

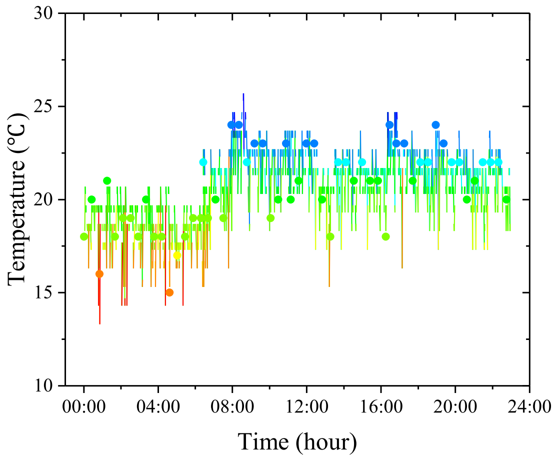

Fig. 9. Temperature of the on-site power cable.

cable is constant unless an accident occurred. Therefore, the amount of heat generated was proportional to the amount of current flowing. The measurement was conducted on August 11, 2019. The maximum and minimum temperatures outside the manhole were 33.9 and 26.4 °C, respectively. However, the manhole is located at a depth of approximately 2–3 m underground; thus, the temperature is considerably lower in summer. The manhole where the system is installed was in a residential area, not in a company or factory area. Before the test, we checked if the local cables were operating normally. Therefore, the temperature of the cable is proportional to the amount of power used. According to the measurement results, power consumption continued to decrease from 12 am to 6 am, and then increased significantly throughout the day. After 19:00 h, the power consumption gradually decreased again. This is similar to the lifestyle of citizens.

The range of the measured temperature change was not large, but the measurable temperature range of the proposed system was from −10 °C to 100 °C, which was sufficient to detect an accident or explosion inside the cable.

3. Conclusion

The temperature of the power cable is a critical monitoring factor in the management of UUTs. It provides information to determine whether the increase is due to the current load or an accident.

This study proposed a sensor module that can monitor the temperature of the power cable joint using a fiber optic sensor. The advantage of using fiber optic sensors is that they are not affected by electromagnetic interference. We built a sensor module consisting of an FBG sensor, a WDM filter, an electronic circuit, and a microprocessor. We could reduce the cost by using a WDM filter to convert the FBG sensor signal to temperature.

The proposed sensor module provides sufficient linearity for field application and can transmit the optical signals far without additional network configurations or power supplies. Therefore, the proposed sensor is expected to be effectively used for temperature monitoring of power distribution grids, especially in long and narrow infrastructures, such as UUTs.

For future work, we plan to apply it to the UUT where there are many cable joints and test it by increasing the number of sensing channels of the proposed module.

CRediT authorship contribution statement

Hyunjin Kim: Experiments, Data analysis, Writing & editing. **Misuk Lee:** Research design, Data analysis, Writing & editing. **Woo-Sug Jung:** Research design, Experiments, Data analysis, Writing & editing. **Seung-Hee Oh:** Research design, Data analysis, Writing & editing.

Declaration of competing interest

The authors declare that they have no known competing financial interests or personal relationships that could have appeared to influence the work reported in this paper.

Acknowledgments

This work was supported by Institute of Information & communications Technology Planning & Evaluation (IITP) grant funded by the Korea government (MSIT, MOIS, MOLIT, MOTIE) (No. 2020-0-00061, Development of integrated platform technology for fire and disaster management in underground utility tunnel based on digital twin)

References

[1] Government of the Republic of Korea, KOREAN NEW DEAL 2.0, 2020, https://www.knewdeal.go.kr/img/img_koreannewdeal_eng.pdf. (Accessed 28 January 2022).

[2] R.F. Wright, P. Lu, J. Devkota, F. Lu, M. Ziomek-Moroz, P.R. Ohodnicki Jr., Corrosion sensors for structural health monitoring of oil and natural gas infrastructure: a review, Sensors 19 (2019) 3964, http://dx.doi.org/10.3390/s19183964.

[3] H. Lu, T. Iseley, S. Behbahani, L. Fu, Leakage detection techniques for oil and gas pipelines: state-of-the-art, Tunn. Undergr. Space Technol. 98 (2020) 103249, http://dx.doi.org/10.1016/j.tust.2019.103249.

[4] A.A. Khan, N. Malik, A. Al-Arainy, S. Alghuwainem, A review of condition monitoring of underground power cables, in: 2012 IEEE International Conference on Condition Monitoring and Diagnosis, 2012, pp. 0909–912, http://dx.doi.org/10.1109/CMD.2012.6416300.

[5] S. Nakamura, S. Morooka, K. Kawasaki, Conductor temperature monitoring system in underground power transmission XLPE cable joints, IEEE Trans. Power Deliv. 7 (1992) 1688–1697, http://dx.doi.org/10.1109/61.156967.

[6] R. Wu, C. Chang, The use of partial discharges as an online monitoring system for underground cable joints, IEEE Trans. Power Deliv. 26 (2011) 1585–1591, http://dx.doi.org/10.1109/TPWRD.2011.2124474.

[7] H. Kim, S. Park, C. Yeo, H. Kang, H. Park, Thermal analysis of 22.9-kV crosslinked polyethylene cable joint based on partial discharge using fiber Bragg grating sensors, Opt. Eng. 60 (2021) 034101, http://dx.doi.org/10.1117/1.OE.60.3.034101.

[8] K.O. Hill, G. Meltz, Fiber bragg grating technology fundamentals and overview, J. Lightwave Technol. 15 (1997) 1263–1276, http://dx.doi.org/10.1109/50.618320.

[9] H. Park, M. Song, Linear FBG temperature sensor interrogation with Fabry–Perot ITU multi-wavelength reference, Sensors 8 (2008) 6769–6776, http://dx.doi.org/10.3390/s8106769.

[10] H. Kim, U. Sampath, M. Song, Multi-stress monitoring system with fiber-optic mandrels and fiber bragg grating sensors in a Sagnac loop, Sensors 15 (2015) 18579–18586, http://dx.doi.org/10.3390/s150818579.

[11] H. Kim, M. Song, A fiber laser spectrometer demodulation of fiber bragg grating sensors for measurement linearity enhancement, J. Opt. Soc. Korea 1 (2013) 312–316, http://dx.doi.org/10.3807/josk.2013.17.4.312.

[12] M. Burunkaya, M. Yucel, Measurement and control of an incubator temperature by using conventional methods and fiber bragg grating (FBG) based temperature sensors, J. Med. Syst. 44 (2020) 178, http://dx.doi.org/10.1007/s10916-020-01650-2.

[13] M. Yucel, N.F. Ozturk, Real-time monitoring of railroad track tension using a fiber bragg grating-based strain sensor, Instrum. Sci. Technol. 46 (2018) 519–533, http://dx.doi.org/10.1080/10739149.2017.1415930.

[14] S.M. Melle, K. Liu, R.M. Measures, A passive wavelength demodulation system for guided-wave bragg grating sensors, IEEE Photon. Technol. Lett. 4 (1992) 516–518, http://dx.doi.org/10.1109/68.136506.

[15] Y. Sano, T. Yoshino, Fast optical wavelength interrogator employing arrayed waveguide grating for distributed fiber Bragg grating sensors, J. Lightwave Technol. 21 (2003) 132–139, http://dx.doi.org/10.1109/JLT.2003.808620.